Published in final edited form as:
Cell Signal. 2014 April ; 26(4): 766–776. doi:10.1016/j.cellsig.2014.01.001.

Arrestin-3 binds the MAP kinase JNK3α2 *via* multiple sites on both domains

Xuanzhi Zhan, **Alejandro Perez**, **Luis E. Gimenez**, **Sergey A. Vishnivetskiy**, and **Vsevolod V. Gurevich***
Department of Pharmacology, Vanderbilt University, Nashville, TN 37232, USA

Abstract

Although arrestins bind dozens of non-receptor partners, the interaction sites for most signaling proteins remain unknown. Here we report the identification of arrestin-3 elements involved in binding MAP kinase JNK3α2. Using purified JNK3α2 and MBP fusions containing separated arrestin-3 domains and peptides exposed on the non-receptor-binding surface of arrestin-3 we showed that both domains bind JNK3α2 and identified one element on the N-domain and two on the C-domain that directly interact with JNK3α2. Using *in vitro* competition we confirmed that JNK3α2 engages identified N-domain element and one of the C-domain peptides in the full-length arrestin-3. The 25-amino acid N-domain element has the highest affinity for JNK3α2, suggesting that it is the key site for JNK3α2 docking. The identification of elements involved in protein-protein interactions paves the way to targeted redesign of signaling proteins to modulate cell signaling in desired ways. The tools and methods developed here to elucidate the molecular mechanism of arrestin-3 interactions with JNK3α2 are suitable for mapping of arrestin-3 sites involved in interactions with other partners.

Keywords

Arrestin; JNK3; protein-protein interactions; MAP kinases; phosphorylation

Introduction

In addition to their best known function as the terminators of G protein-coupled receptor (GPCR) signaling *via* G proteins [1, 2], the two non-visual arrestins, arrestin-2[1] and -3, have recently emerged as multi-functional adaptors regulating different cellular processes, including mitogen-activated protein kinase (MAPK) activation [3–5], chemotaxis [6],

*Correspondence to: Vsevolod V. Gurevich, Department of Pharmacology, Vanderbilt University, Nashville, TN 37232, USA; vsevolod.gurevich@vanderbilt.edu.

Contributors
XZ, AP, LEG, and SAV performed experiments; XZ, LEG, and VVG designed the study and wrote the manuscript. All authors have approved the final article.

Conflict of interest
The authors declare no conflict of interest.

[1]We use the systematic names of arrestin proteins: arrestin-1 (historic names S-antigen, 48 kDa protein, visual or rod arrestin), arrestin-2 (β-arrestin or β-arrestin1), arrestin-3 (β-arrestin2 or hTHY-ARRX), and arrestin-4 (cone or X-arrestin; for unclear reasons its gene is called "*arrestin 3*" in the HUGO database).

apoptosis [7], and protein ubiquitination [8, 9]. Dozens of arrestin-binding proteins have been identified recently [10]. Arrestin partners demonstrate great diversity both structurally and functionally [10, 11]. Although arrestins often tether several components to form a signalosome, the size of arrestins (~45 kDa) suggests that they cannot accommodate more than 4–5 partners simultaneously [2]. Therefore, arrestin has to make the "decision" to bind the right partners in various physiological conditions [2, 12]. However, how arrestins selectively associate with the appropriate partners remains a challenging question.

The c-Jun NH_2-terminal protein kinases (JNKs), members of MAPK family, play critical roles in regulating cell fate and were implicated in a multitude of diseases ranging from cancer to neurological and immunological/inflammatory disorders [13]. Like other MAPKs, JNKs are activated *via* three-component cascade conserved in all eukaryotes, in which the kinases successively phosphorylate and activate downstream enzymes [14]. JNK activation often involves scaffold proteins [15, 16]. Arrestin-3 facilitates of a long JNK3 isoform JNK3α2 by directly tethering ASK1, MKK4, and JNK3α2 to form a complete signaling complex [3, 17–19]. We recently found that arrestin-3 can recruit another upstream kinase MKK7 to phosphorylate the threonine site in the T-X-Y motif of JNK3 [19], as well as JNK1/2 isoforms [20]. Although the scaffolding function of arrestins in JNK3 and other MAPK activation has been appreciated in recent years, the molecular mechanism of arrestin-dependent activation of MAP kinases remains to be elucidated. In particular, arrestin sites mediating the binding of each kinase remain unknown [21]. In fact, most of the binding sites of non-receptor partners on arrestin have not been identified yet [22]. Regarding JNK3 binding, previously identified arrestin-3-specific sequence that was proposed to mediate exclusive JNK3 interaction [23] was found to be unique for the rodent proteins [11], while arrestins from other species that do not have that sequence also bind JNK3 and promote its activation [17–20, 24–26]. Even though the original study suggested that arrestin-3 promotes JNK3 phosphorylation in response to receptor activation [3], it was subsequently shown by the same group [23] and others [17, 26] that arrestin-3-mediated JNK3 activation in cells does not depend on GPCRs. Moreover, purified arrestin-3 in the absence of receptors was shown to facilitate the phosphorylation of different JNK isoforms by MKK4 and MKK7 [18–20]. Thus, it remained unclear whether receptor-bound arrestin-3 can interact with JNKs, i.e., whether the binding sites for GPCRs and JNK3 overlap.

Here, we directly tested for the first time the interaction of receptor-bound arrestin-3 with JNK3α2. The spin-down assay with purified proteins, as well as BRET-based interaction assay in intact cells unambiguously demonstrated that JNK3α2 directly associates with receptor-bound arrestin-3, suggesting that JNK3 binding site(s) must be localized on the non-receptor-binding surface of arrestin-3. In order to identify JNK3 binding site(s), we constructed and purified a set of maltose binding protein (MBP) fusions containing either a fragment of arrestin-3 from the non-receptor-binding side, or a single domain of arrestin-3. We measured and compared the binding of these MBP-fusion proteins with JNK3α2. Three fragments located on both domains were found to bind JNK3α2 directly. Two out of these three peptides inhibit the interaction between full-length arrestin-3 and JNK3α2, indicating that these peptides compete for the binding sites on JNK3α2 used by arrestin-3. The methods and molecular tools described here can be used to identify arrestin-3 docking sites of other non-receptor binding partners to gain an insight into the structural basis of their interaction with arrestins.

Materials and methods

Materials

All restriction and DNA modifying enzymes (T4 DNA ligase, Vent DNA polymerase, and calf intestine alkaline phosphatase) were from New England Biolabs (Ipswich, MA). The

luciferase substrate coelenterazine-*h* was obtained from NanoLight Technology (Pinetop, AZ). Other chemicals were from sources recently described [19, 20].

Bioluminescence resonance energy transfer (BRET) assay

BRET-based [27, 28] protein-protein interaction assays were performed to assess the arrestin-mediated interaction of JNK3α2 with angiotensin II receptor type I (AT1R) following the procedure used for the arrestin-receptor interaction assay [26, 29, 30]. Cultured COS-7 cells were reseeded into 60 mm dishes 24 h before transfection in complete DMEM medium (Mediatech-Corning, Manassas, VA). Plated cells were transfected with Lipofectamine 2000 (Life Technologies) following the manufacturer's instructions with AT1R-*R*Luc8 (AT1R fused to *Renilla* luciferase variant 8 at the C-terminus) coding plasmid (0.6 μg/dish), bovine arrestin-3 (0–6 μg/dish) and Venus N-terminus-tagged JNK3α2 (3 μg/dish). Cells were transferred to white opaque 96 well plates and luminescence at 460 and 535 nm was measured 48 h post-transfection. Cells were stimulated by 1 μM angiotensin II (agonist) or vehicle (control) followed by the addition of 5 μM coelenterazine-*h* (*Renilla* luciferase substrate). Measurements were taken at 10-minute intervals for up to 90 minutes. Angiotensin-induced net BRET was determined by subtracting the 535 nm/460 nm BRET ratio in the absence of agonist from the ratio of agonist-treated cells for each arrestin concentration. Results are expressed as the net BRET values for each amount of arrestin-3 at a given time point after agonist stimulation.

Immunoprecipitation

Binding of JNK3α2 to AT1R-bound arrestin-3 was measured by co-immunoprecipitation. HEK-293A cells were co-transfected with HA-tagged AT1R-*R*luc8, Flag-JNK3α2, and GRK2 with or without arrestin-3. 48 h after transfection, cells in 60-mm plates were lysed in 0.4 ml of lysis buffer (50 mM Tris, 2 mM EDTA, 250 mM NaCl, 10% glycerol, 0.5% Nonidet P-40, 20 mM NaF, 1 mM Na orthovanadate, 10 mM N-ethylmaleimide, 2 mM benzamidine, and 1 mM phenylmethylsulfonyl fluoride) for 30 min at 4°C. After centrifugation, supernatants were pre-cleared by 30 μl of protein G agarose. Then 700 μl of lysates (combined from two 60 mm plates) were incubated with anti-HA (rat, Roche) antibody overnight followed by the addition of 30 μl of protein G agarose. The suspensions were transferred to centrifuge filters (Ultrafree, Millipore) and washed three times with 300 μl of lysis buffer. Proteins were eluted with 35 μl of SDS sample buffer and analyzed by Western blot.

Purification of arrestin-3 and JNK3α2-His

Arrestin-3 was purified as previously described [31, 32]. Briefly, untagged bovine arrestin-3 was expressed in *Escherichia coli* and purified by sequential Heparin-Sepharose and Q-Sepharose chromatography to >95% purity, as judged by Coomassie staining of SDS PAGE gel. C-terminal His6-tagged JNK3α2 was purified as previously described with minor modifications [18, 19]. Briefly, JNK3α2-His was expressed in *Escherichia coli* and purified by sequential Ni-NTA and phenyl-Sepharose chromatography to >90% purity, as judged by Coomassie staining.

Rhodopsin preparation, phosphorylation, and regeneration

Urea-treated bovine rod outer segment membranes were prepared, phosphorylated with endogenous rhodopsin kinase, and regenerated with 11-cis-retinal, as described [33]. The ability of prepared phospho-rhodopsin to bind arrestins upon light activation was tested in direct binding assay with visual arrestin-1, as described [34, 35].

MBP-fusion protein constructs in pMal

To make MBP-fusions containing arrestin-3 elements (MBPT1, 2A, 2B, 3–7, (cf. Fig. 3.)), the cDNAs encoding different arrestin-3 fragments were subcloned into pMal-p2T (generous gift from Dr. Keiji Tanaka, Tokyo Institute of Medical Science) between Eco RI and Xho I sites in frame with MBP. MBP-Arr3 (full-length arrestin-3), MBP-A3N (arrestin-3 N-domain), and MBP-A3C (arrestin-3 C-domain) were created by subcloning the corresponding cDNA into pMal-p2T between Eco RI and Not I sites. All MBP-arrestin-3 fusion proteins contained the same TLVPRGSPGF linker between MBP and arrestin-3 or its fragments. The MBP protein used as negative control was purified using empty pMal-p2T vector containing the same linker with 10 additional residues: PGRLERPHRD (Fig. 3C).

Expression and purification of MBP-fusion proteins

The MBP-fusion proteins containing arrestin-3 fragments were expressed and purified following previously described protocol for MBP-Arr3 with minor modifications [19, 20]. MBP proteins were expressed in *Escherichia coli* (BL21-codon plus (DE3)-RIL). Cells were grown overnight at 30°C, then induced with 1 mM isopropyl β-D-thiogalactoside for 5–6 h. The MBP proteins were purified using amylose beads (50% slurry, NEB) and batch protocol, according to the manufacture's manual. The proteins were eluted with a buffer containing 50 mM maltose. The eluates were dialyzed three times (>3 h each time) to remove maltose. The purified protein samples were concentrated to 0.2–1 mg/ml, and stored at −80°C until further use.

Rhodopsin spin-down assay

Binding of JNK3α2 to rhodopsin-bound arrestin-3 was measured by the rhodopsin spin-down assay with light-activated phosphorylated rhodopsin (P-Rh*) carrying more than three moles of phosphate per mole of rhodopsin [33] in native disc membranes, as described [36, 37]. Arrestin-3 (3 μg) was pre-mixed with unphosphorylated rhodopsin (Rh, 5 μg), phosphorylated rhodopsin (P-Rh, 5 μg), or binding buffer (50 mM HEPES-Na, pH 7.3, 150 mM NaCl) in a final volume of 50 μl in the dark. Rhodopsin was activated by bright light for 10 min at 30°C. The samples were immediately placed into centrifuge filters (Millipore, Durapore-PVDF 0.65 μm; catalogue # UFC30DV00) and spun at 2,500 x g for 20 s to separate the supernatants from the rhodopsin-containing membranes. Rhodopsin-containing membranes were washed with 300 μl binding buffer three times. 30 μl SDS sample buffer was added to dissolve the membranes. The proteins were resolved using 10% SDS-PAGE and stained by Coomassie blue. The binding of JNK3α2 to rhodopsin-bound arrestin-3 was also measured by a modified spin-down assay. The solutions containing 3 μg of arrestin-3 with purified JNK3α2 (1 or 3 μg) were pre-mixed with phosphorylated rhodopsin in the dark, with the same amounts of JNK3α2 mixed with rhodopsin in the absence of arrestin-3 serving as negative controls. After light activation of rhodopsin for 10 min at 30°C, the samples were immediately transferred to the centrifuge filters. Rhodopsin-containing membranes were separated from the supernatant by centrifugation (2,500 x g, 20 s) and washed with 300 μl of binding buffer three times. Rhodopsin-bound arrestin-3 was eluted from membranes with the elution buffer (2 M NaCl, 50 mM HEPES, pH 7.3) after incubation for 2 h at 4°C. JNK3α2 in the eluate was detected by Western blot. Membrane pellets were dissolved in 30 μl SDS sample buffer. The proteins in eluates and membrane samples were resolved using 10% SDS-PAGE and stained by Coomassie blue.

His-tag pull-down

Identification of arrestin-3 fragments capable of binding JNK3α2 was performed by His-tag pull-down with JNK3α2-His immobilized on Ni-NTA agarose resin, 50 μl of purified JNK3α2-His (5 μg) were incubated with 25 μl Ni-NTA resin (50% slurry) in binding buffer

(50 mM HEPES-Na, pH 7.3, 150 mM NaCl, 50 mM imidazole) at 4°C with gentle rotation for 2 h. The final mixtures contained 0.6 μM JNK3α2-His; the final concentrations of MBP-fusions (5 μg) were: 0.6–0.67 μM of MBP-T1-T7, 0.48 μM of MBP-A3N, 0.43 μM of MBP-A3C, and 0.34 μM of MBP-A3. The suspensions were transferred to centrifuge filters and washed three times with binding buffer. The proteins were eluted by the addition of 100 μl of elution buffer (250 mM imidazole, 50 mM HEPES-Na, pH 7.3, and 150 mM NaCl). Eluates were analyzed by SDS PAGE and Western blotting.

MBP pull-down

MBP pull-down was also employed to identify arrestin-3 fragments that bind JNK3. MBP-fusion proteins (5 μg in 100 μl) were immobilized on amylose resin (25 μl, 50% slurry, NEB) by incubating at 4°C with gentle rotation for 2 h. The final mixtures contained 0.60 μM of JNK3α2-His; the final concentrations for MBP fusions were: 0.60~0.67 μM of MBP-T1-7, 0.48 μM of MBP-A3N, 0.43 μM of MBP-A3C, and 0.34 μM of MBP-A3. Then 50 μl of JNK3α2 (5 μg) were added and incubated at 4°C for 2 h. Each suspension was transferred to centrifuge filters and washed three times with 50 mM HEPES-Na, pH 7.3, 150 mM NaCl. The proteins were eluted by 100 μl of elution buffer (wash buffer containing 50 mM maltose). Eluates were analyzed by SDS-PAGE and Western blotting.

Quantification and Statistical Analysis

The bands on the X-ray film were quantified using Quantity One software (Bio-Rad). Repeated measures ANCOVA (StatView software, SAS Institute) was used for statistical analysis of quantitative data; $p < 0.05$ was considered significant.

Results

JNK3α2 binds receptor-associated arrestin-3

Although arrestin-3 was originally shown to function as a receptor-regulated scaffold for JNK3 activation [3], follow-up studies indicated that receptor stimulation is not obligatory for this arrestin-3 function: over-expression of upstream kinases ASK1 [17, 23, 26], MKK4 or MKK7 [19] facilitates JNK3α2 activation without receptor stimulation, and an arrestin-3 mutant with a seven-residue deletion in the inter-domain hinge (Δ7), which severely impedes receptor binding [38, 39], was shown to effectively promote JNK3 phosphorylation in cells [17, 26]. Facilitation by purified arrestin-3 of MKK4/7-mediated JNK3α2 phosphorylation *in vitro* proved that free arrestin-3 can serve as a scaffold for MKK4/7-JNK3α2 signaling modules [18, 19]. Receptor binding induces global conformational change in arrestins [36, 40–43]. This rearrangement likely alters the set of exposed elements, thereby affecting the association of non-receptor binding partners [12]. Previous studies indicated that JNK3α2 comparably binds arrestins in different conformations mimicked by mutations that make arrestins constitutively active (such as the triple alanine substitution in the C-tail that forcibly detaches it from the body of the molecule, 3A [44–47]) or “frozen” in the basal state (such as Δ7) [24, 26]. While ERK2 was shown to interact with receptor-bound arrestins [37], the evidence that JNK3α2 can directly associate with receptor-bound arrestin-3 was never reported.

To address this issue, we developed a direct spin-down assay using purified arrestin-3 bound to active phosphorylated rhodopsin (P-Rh*) to pull-down JNK3α2. We first tested the binding of arrestin-3 to P-Rh* under these conditions, with the same amount of unphosphorylated active rhodopsin (Rh*) serving as a control. In full agreement with previous studies [39, 45, 47], we found that P-Rh* binds the majority of arrestin-3, whereas Rh* demonstrated a much lower binding (Fig. 1A). These results proved that pelleted arrestin-3 was specifically bound to P-Rh*, rather than non-specifically associated with the

membranes. To evaluate JNK3α2 binding to receptor-associated arrestin-3, we mixed purified P-Rh*, arrestin-3, and JNK3α2, pelleted the membranes after brief incubation sufficient for the binding of the majority of arrestin-3 (Fig. 1A), and then eluted receptor-bound arrestin-3 along with associated proteins using high-salt buffer (20 mM Tris, pH 7.5, 2 M NaCl). JNK3α2 in these samples was detected by Western blot (Fig. 1B). We found that high salt elutes bound arrestin [48, 49], that P-Rh*-associated arrestin-3 recruits JNK3α2, whereas no JNK3α2 was detected in samples where arrestin-3 was omitted (Fig. 1B).

To confirm JNK3 interaction with arrestin-3 associated with non-visual receptors, we used two complementary approaches. First, we used in cell BRET-based interaction assay between *Renilla* luciferase-tagged angiotensin II receptor type I (AT1R) and N-terminally Venus-tagged JNK3α2 in the presence of varying amounts of expressed arrestin-3 (Fig. 2). Free arrestin-3 was shown to directly bind JNK3α2 by several methods [18–20, 26]. Upon agonist activation AT1R was shown to bind arrestin-3 with high affinity [50]. Therefore, if receptor-bound arrestin-3 retains the ability to associate with JNK3α2, we expected it to co-recruit JNK3α2 to agonist-activated AT1R, which would result in energy transfer from receptor-attached RLuc to JNK3α2-attached Venus (Fig. 2A). The net BRET (increase in BRET signal upon angiotensin II addition) in cells that were co-transfected with varying amounts of bovine arrestin-3 was measured at 10-min time-point intervals (Fig. 2B). Net BRET after 10 min yielded a modest increase in this value. However, 20 min or longer exposure to the agonist produced significantly higher net BRET values (Fig. 2B). Importantly, the increase in net BRET peaked at modest arrestin-3 expression (Fig. 2B, C) and decreased at higher arrestin-3 levels. This biphasic dependence of signal on arrestin-3 concentration is consistent with arrestin-3 serving as a scaffold bringing AT1R and JNK3α2 together: the excess of the scaffold promotes the formation of incomplete complexes containing only one of the partners, as was predicted by mathematical modeling [51, 52] and recently demonstrated experimentally [18–20]. Second, we confirmed that arrestin-3 brings JNK3α2 into complex with AT1R by co-immunoprecipitation (Fig. 2E). To this end, we co-expressed AT1R and JNK3α2 in the presence and absence of arrestin-3, and found that JNK3α2 co-immunoprecipitates with AT1R only in the presence of arrestin-3 (Fig. 2E).

Thus, three independent lines of evidence, *in vitro* spin-down (Fig. 1), BRET in intact cells (Fig. 2A–D), and co-immunoprecipitation (Fig. 2E) invariably show that receptor-bound arrestin-3 retains the ability to interact with JNK3α2. Importantly, the same results were obtained using model receptor P-Rh* with purified proteins (Fig. 1) and AT1R in intact cells (Fig. 2). To the best of our knowledge, this is the first direct experimental evidence that the receptor-arrestin-3 complex binds JNK3α2. These data show that JNK3α2 interacts with the non-receptor-binding side of arrestin-3.

Arrestin-3 interacts with JNK3α2 via multiple sites

Arrestin-3 is believed to facilitate phosphorylation of JNK3α2 via simultaneous binding of each kinase in the ASK1-MKK4-JNK3α2 cascade [17, 22]. Structurally, arrestin-3 is an elongated molecule consisting of the N- and C-domains (Fig. 3A) [31], with the overall fold very similar to that of other arrestin subtypes [53–57]. Numerous studies by many groups using a variety of methods demonstrated that GPCRs engage the concave sides of the two arrestin domains [34–36, 41, 43, 58–67]. Thus, in the receptor-bound arrestin-3 the concave sides of both domains were occupied by receptor. The fact that JNK3α2 interacts with the receptor-bound arrestin-3 suggests that JNK3α2 binds to the non-receptor-binding surface of arrestin-3 (Fig. 3B). Based on these considerations and direct evidence that JNK3α2 indeed associates with receptor-bound arrestin-3 (Figs. 1,2), to identify arrestin-3 elements that mediate its interaction with JNK3α2, we constructed a series of MBP-fusion proteins

containing peptides exposed on the non-receptor-binding side of arrestin-3 (Fig. 3). Eight arrestin-3 fragments were selected based on their location and secondary structure (Fig. 3A, B). Collectively these arrestin-3 fragments, varying from 14 to 64 residues (Fig. 3C), cover the surface of arrestin-3 that is not occupied by the receptor. Separated N- and C-domains of arrestin-3 were reported to co-immunoprecipitate with JNK3α2 from co-expressing cells [17]. However, immunoprecipitation was performed from total cell lysates, where dozens of arrestin-3 and/or JNK3α2 binding partners could have mediated the association between individual arrestin-3 domains and JNK3α2. Therefore, we also constructed and purified MBP-fusions containing individual N- and C-domains of arrestin-3 (MBP-A3N and MBP-A3C) to evaluate their interactions with JNK3α2 using purified proteins. The purity of MBP-fusion proteins generated is shown in Fig. 3D.

To map the JNK3α2 binding sites on arrestin-3, we first performed a His-tag pull-down by testing which MBP-fusions bind to immobilized JNK3α2-His (Fig. 4A). The same amounts of MBP and MBP-arrestin-3 proteins were used as negative and positive controls, respectively. No non-specific binding of MBP itself was observed, and the specific interaction between JNK3α2 and MBP-arrestin-3 was readily detected, as expected. In agreement with a previous report [17], both N- and C- domains of arrestin-3 were retained by JNK3α2 (Fig. 4A), suggesting that JNK3α2 engages more than one site, and that these sites are localized on both domains. In addition, three arrestin-3 fragments were also retained by JNK3α2: T1 from the N-domain and T3 and T6 from the C-domain (Fig. 4A). MBP-T1 demonstrated the strongest binding, and no other N-domain element (T2A, T2B) was retained by immobilized JNK3α2. Thus, the T1 fragment representing the first 52 residues is the primary JNK3α2 binding site in the N-domain. Even though both domains demonstrated similar binding to JNK3α2, no individual fragment from the C-domain interacted with JNK3α2 as strongly as T1 (Fig. 4A). Instead, two elements (T3 and T6) demonstrated modest JNK3α2 binding. Thus, JNK3α2 binding site on the C-domain likely consists of separate parts, in contrast to the compact site on the N-domain. Out of the two C-domain elements contributing to JNK3α2 interaction, T6 demonstrated stronger binding than T3 (Fig. 4A).

To further confirm these observations, we also performed the reverse pull-down assay, using immobilized MBP proteins to trap JNK3α2. As shown in Fig. 4B, the results of the MBP pull-down were in full agreement with the His-tag pull-down assay. JNK3α2 bound MBP-arrestin-3 and both separated domains, as expected. JNK3α2 was also retained by T1, T3, and T6, with MBP-T1 showing the strongest binding (Fig. 4B). Thus, direct pull-down with purified proteins performed both ways identified the same three JNK3α2 binding sites on the non-receptor side of arrestin-3.

The first 25 residues are the primary JNK3α2 binding site in the N-domain

The first 52 residues of arrestin-3 (T1) apparently serve as the primary JNK3α2 binding site in the N-domain (Fig. 4). Interestingly, this region was previously reported as the binding site for the upstream kinase ASK1 (kinase domain) by a scanning peptide array approach [68]. The β-strand I within the T1 fragment is an essential part of the three-element interaction involving β-strand I, α-helix I, and the C-tail, which was shown to hold all arrestins in their basal conformation [31, 54, 55, 57]. The disruption of this interaction by targeted mutations greatly increases the conformational flexibility of arrestins [46] and their binding to all forms of their cognate receptors, including unpreferred active unphosphorylated and inactive phosphorylated [34, 35, 44, 45, 47, 69–72]. In both His-tag and MBP pull-down assays, MBP-T1 demonstrated the strongest binding among all fragments tested (Fig. 4A, B). To further identify the JNK3α2 binding elements in this region, we constructed three new MBP-fusions containing parts of the T1 peptide: MBP-T1A (residues 1–25), MBP-T1B (26–52) and MBP-T1C (16–45) (Fig. 5A). The interaction

of these fragments with JNK3α2 was analyzed using His-tag pull-down. Both MBP-T1A and MBP-T1C interacted with JNK3α2, whereas MBP-T1B did not bind JNK3α2. Quantification revealed that the amounts of MBP-T1A and MBP-T1C retained by the same amount of JNK3α2 were ~85% and ~10% of that of MBP-T1, respectively (Fig. 5C). Thus, a part of the T1 representing the first 25 residues of arrestin-3 (T1A) constitutes the primary JNK3α2 binding site in the N-domain of arrestin-3.

T1A and T6 peptides compete with arrestin-3 for JNK3α2

It is possible that short peptides fused to MBP do not fold into the same conformation as in full-length arrestin-3, and therefore can interact with other proteins non-specifically. Therefore, to ascertain the specificity of observed interactions, it is necessary to test whether identified elements, T1A, T3, and T6, mediate JNK3α2 binding in properly folded full-length arrestin-3. To this end, we performed a competition pull-down to determine whether these individual peptides compete with full-length arrestin-3 for JNK3α2 (Fig. 6). Both MBP-T1A and MBP-T6 demonstrated dose-dependent inhibition of arrestin-3 binding to JNK3α2. No inhibition was observed in the case of MBP-T3 at the concentrations tested, up to 30 μg per assay (Fig. 6), in agreement with the weakest binding of this peptide to JNK3α2 (Fig. 4). In this assay, 10 μg of MBP-T1A more significantly inhibited arrestin3-JNK3α2 interaction than 20 μg of MBP-T6. The efficiency of inhibition by individual peptides in this paradigm was in full agreement with their ability to bind JNK3α2 directly measured in earlier pull-down assays (Figs. 4,5). MBP-T1A that demonstrated the strongest binding (Fig. 5) was found to be the most effective inhibitor (Fig. 6). Thus, both arrestin-3 peptides that showed stronger binding to JNK3α2 were found to significantly inhibit the interaction between arrestin-3 and JNK3α2. This competition demonstrates that in properly folded full-length arrestin-3 JNK3α2 engages the elements represented by the identified T1A and T6 peptides, whereas unambiguous conclusions regarding the role of T3 peptide in the interaction cannot be made.

Discussion

Arrestins provide versatile signaling platforms and regulate multiple cellular functions because of their ability to bind dozens of diverse partners [21, 73]. The two ubiquitously expressed non-visual arrestins, arrestin-2 and -3 [11, 74, 75] apparently interact with hundreds of GPCRs [76] and numerous non-receptor signaling proteins [10]. In a recent proteomic analysis 71 proteins were reported to bind arrestin-2, 162 proteins bound arrestin-3, and 102 proteins interacted with both non-visual arrestins [10]. Interestingly, some partners prefer receptor-bound arrestin conformation (e.g., ERK1/2 [37], clathrin [77, 78], E3 ubiquitin ligase AIP4 [79]), others preferentially bind arrestins in their basal state (e.g., E3 ubiquitin ligases Mdm2 and parkin [9, 24], as well as Ca^{2+}-liganded calmodulin [80]), whereas some, like JNK3α2, do not show an obvious preference [24]. The scaffolding functions of arrestins for MAPK cascades were discovered less than 15 years ago [3, 4]. Arrestins were reported to facilitate the activation of the three main subfamilies of MAP kinases: JNK [3], ERK [4], and p38 [5]. To facilitate the activation of MAPK, arrestin needs to bind MAPK and its upstream kinases MAPKK and MAPKKK. Precise identification of the binding sites of non-receptor partners on arrestins would provide critical mechanistic insights and enable the construction of designer arrestins with desired signaling bias [21, 22]. Unfortunately, out of hundreds of potential non-receptor interaction partners of arrestins [10], binding sites for very few were mapped with any precision: those for clathrin [77, 81], AP2 [77, 82, 83], microtubules [39, 84], calmodulin [80], PDE4 [85], MEK1 [86], ASK1 and MKK4 [68]. Site identification would be particularly important in exploring the interactions between arrestins and MAP kinases, because to promote signaling arrestins need to assemble very specific combinations of MAPK, MAPKK and MAPKKK. It is not clear

how simultaneous association of mismatched kinases that would yield unproductive complexes is prevented. The first step towards answering these questions must be precise identification of kinase-binding elements on arrestins.

Although arrestin-3 was originally proposed to act as a receptor-regulated scaffold for JNK3α2 activation [3], follow-up studies indicated that free arrestin-3 is capable of performing this function [17–19, 23, 25, 26]. Cell-based nuclear exclusion assay showed that JNK3 comparably binds arrestin-3 in different conformations: basal, constitutively "pre-activated" form (3A mutant) and Δ7 mutant frozen in the basal state [24]. However, in contrast to the interaction between free arrestin-3 and JNK3α2, which has been extensively studied using a battery of cell-based, biochemical, and biophysical methods, including co-IP [3, 17, 20, 25, 26], nuclear exclusion [24], direct pull-down with purified proteins, and FRET [18–20], the effect of receptor binding on arrestin-3 association with JNK3α2 has never been directly evaluated. The idea that receptor-bound arrestin-3 can associate with JNK3α2 remained no more than a plausible, but unsubstantiated hypothesis [3, 12]. Here we employed three different approaches to test whether receptor-bound arrestin-3 retains the ability to bind JNK3α2. First, using purified proteins, we demonstrated that JNK3α2 directly binds the rhodopsin-arrestin-3 complex, but not free rhodopsin (Fig. 1). Second, we showed that optimal arrestin-3 expression levels promote JNK3α2 association with AT1R in intact cells upon agonist stimulation (Fig 2A–D). Finally, we found that JNK3α2 co-immunoprecipitation with AT1R is strictly dependent on the co-expression of arrestin-3 (Fig. 2E). These data represent the most unambiguous evidence reported thus far, that receptor-associated arrestin-3 binds JNK3α2. These results also clearly show that JNK3α2 interacts with the non-receptor-binding side of arrestin-3, as was previously hypothesized [12].

Numerous lines of evidence suggest that receptor-induced conformational change in arrestins involves the movement of the two domains relative to each other [36, 38, 39, 43, 87, 88]. Therefore, it would seem natural for proteins sensitive to arrestin conformation to engage both arrestin domains, as has been shown for cRaf1 and ERK2 [17]. This prediction cannot be made in case of JNK3α2, which comparably binds arrestins in different conformations [24]. Therefore, in search of JNK3α2 binding site we scanned the convex non-receptor-binding surface of both domains (Fig. 3). MBP fusion peptides were previously used for generating peptide inhibitors and substrates [89] and for identification of elements with high binding affinity for rhodopsin [90]. We employed this strategy by generating MBP-fusion proteins containing a series of arrestin-3 peptides. To minimize the probability of misfolding, we selected fragments in such a way as not to interrupt stretches of secondary structure (Fig. 3). Because all peptides were fused to the same protein, MBP, we were able to compare the relative binding of these peptides to JNK3α2 in a semi-quantitative pull-down assay (Figs. 4, 5). Since all assays were carried out *in vitro* with pure proteins, we could exclude the participation of and/or any interference from other proteins, which is always a possibility in case of co-immunoprecipitation from cell lysates, which contain hundreds of different proteins. The two arrestin domains are independent folding units, which retain certain functions [9, 17, 48, 59, 60, 91, 92]. Therefore, for comparison we also generated MBP fusions containing full-length arrestin-3 and its separated N- and C-domains. Our results confirmed previous observations that individual domains of arrestin-3 bound JNK3α2 with comparable affinity. We also identified three JNK3α2 binding peptides, T1 (narrowed to T1A) from the N-domain, as well as T3 and T6 from the C-domain (Figs. 4, 5). T1A contains the first 25 residues of arrestin-3 and appears to serve as the primary JNK3α2 binding site on the N-domain, while the binding site on the C-domain consists of at least two elements, T3 and T6, both of which demonstrated much lower affinity for JNK3α2 than T1A (Figs. 4–6).

Since the accessibility of a separated peptide is usually much greater than of the same sequence incorporated in a protein, it was important to ascertain that the elements identified by pull-down assays are actually engaged by JNK3α2 in the full-length arrestin-3. If this were the case, the peptides would be expected to compete with arrestin-3 for JNK3α2. Indeed, we found that both T1A and T6 peptides inhibited the interaction between full-length arrestin-3 and JNK3α2 in a dose-dependent manner (Fig. 6), which is consistent with direct competition. The inhibition by T3 was not observed under the conditions tested, which could be due to very low affinity of T3 for JNK3α2 (Fig. 4).

The two non-visual arrestins are highly homologous [74, 75], yet in contrast to arrestin-3, arrestin-2 does not promote JNK3α2 activation in cells [3, 17, 23]. To identify arrestin-3-specific residues responsible for the ability to facilitate JNK3α2 activation, in a previous study arrestin-3 residues were replaced with homologous residues of arrestin-2 [25]. As expected, several substitutions significantly reduced arrestin-3-dependent JNK3α2 phosphorylation in cells [25]. Interestingly, all of the residues identified as critical for JNK3α2 activation were localized in the C-domain: Val-343 was found to be the key contributor to this function, whereas Leu-278, Ser-280, His-350, Asp-351, His-352, and Ile-353 played supporting role [25]. These residues are contained in the T5 and T7 peptides, neither of which demonstrated detectable JNK3α2 binding (Figs. 3,4). These data suggest that, as far as JNK3α2 activation is concerned, critical differences between arrestin-2 and -3 lie not in their interactions with JNK3α2, but either in the binding of the upstream kinases, or in the relative orientation of the three kinases in the complex. The fact that arrestin-3 mutants with very different ability to facilitate JNK3α2 activation tested in two recent studies [25, 26] showed comparable binding to ASK1, MKK4, and JNK3α2 suggests that relative orientation plays more important role that binding affinity.

JNK3 is a neuron-specific isoform of JNKs, which has been implicated in neurodegenerative diseases, such as Parkinson's [93], Alzheimer's [94, 95] and Huntington's [96]. These studies suggest that regulation of JNK3 activity could be a promising therapeutic intervention for neurodegenerative diseases. Previously, several arrestin-3 mutants were described that bind JNK3α2 and its upstream kinases (MKK4 and ASK1) at least as well as wild-type arrestin-3 but fail to facilitate the activation of JNK3 [25, 26]. These observations led to the construction of a silent scaffold: arrestin-3 KNC mutant that demonstrated a stronger binding to JNK3 than WT, retained normal MKK4 and ASK1 binding, but suppressed JNK3 activity by sequestering JNK3 and its upstream kinases away from productive scaffolds [26]. Engineering of molecular tools of this type creates new methods for precise regulation of JNK3 activity [21, 22]. As key regulators of JNK signaling, scaffold proteins modulate spatial and temporal activation of JNK, and their re-engineered versions can serve as more specific inhibitors than small molecules. Compared to the ubiquitously expressed JNK1 and JNK2, the neuron-specific JNK3 is a "safer" therapeutic target. The most successful strategy to design JNK3-specific inhibitors is by targeting its scaffold proteins, such as JIP [97]. Arrestin-3-derived JNK3-binding peptides identified here have potential to become novel tools to target and specifically manipulate JNK3 activation *via* arrestin-3 and other scaffolds.

To regulate the activity of dozens of fairly diverse partners, arrestin has to make "decisions" to selectively bind the right proteins at the right time. These decisions can be affected by the cellular location, conformation, local concentration of arrestins and their binding partners, as well as other factors. In particular, binding-induced conformational changes in arrestin can play a decisive role in arrestin-mediated assembly of distinct signaling complexes in various physiological conditions [12]. The crystal structures of the basal conformation of all four mammalian arrestin subtypes revealed a remarkably similar fold, particularly in the core of both domains [31, 53–57]. Several recent studies attempted to determine receptor-bound

"active" conformation of arrestins using various methods, including NMR [43], EPR [36], and crystallization [87, 88]. Even though each of these approaches has obvious caveats, such as the lack of atomic resolution in biophysical studies of arrestin complexes with real receptor [36, 43], and the absence of real receptor in reported structures of "active" arrestins [87, 88], collectively these studies proved very informative. Not surprisingly, every study detected significant conformational rearrangements in arrestins. EPR allowed to document the movement of several flexible loops on the receptor-binding side of the molecule [36], some of which were predicted, while others turned out to be quite unexpected. NMR revealed the engagement of distinct arrestin elements by different functional forms of the receptor (which was predicted earlier based on mutagenesis and EPR data [41, 48, 60–62]), and global increase in arrestin flexibility upon the binding to active phosphorylated receptor [43]. Overall "loosening up" of the arrestin structure upon receptor binding was never predicted, although it makes sense biologically: receptor-bound arrestin is expected to interact with numerous signaling proteins, and in many cases unstructured elements mediate protein-protein interactions *via* coupled binding and folding mechanism [98, 99]. It was suggested that a global conformational change in arrestins induced by receptor binding [40, 48] includes the movement of the two domains relative to each other [100]. This idea was supported by the finding that the deletions in the extended inter-domain hinge impair receptor binding of all arrestins [38, 39]. However, the analysis of the conformation of receptor-bound arrestin by measuring distances between pairs of sites within the molecule [36] did not support the model of clam-like movement of the two domains (Fig. 1A) that would grab the receptor like a pincer. Two recent structures, one of truncated form of arrestin-2 (that was shown to be constitutively active previously [47]) associated with multi-phosphorylated C-terminus of vasopressin V2 receptor [88], and the other of short arrestin-1 splice variant p44 also lacking the C-tail [87] are remarkably similar. Both suggest an alternative conformational rearrangement: twisting of the two domains relative to each other by 20–21°. Both structures also showed large movement of the "139 loop" in the central crest of the receptor-binding surface, away from the "finger loop" implicated in receptor binding [41, 66, 101, 102], which was earlier discovered in the EPR study [36] and confirmed by mutagenesis [34]. Because of the absence of the receptor in these structures, we cannot be sure how much the domains actually twist when arrestins bind GPCRs. However, domain rotation nicely explains the hinge deletion results [38, 39] that the EPR study left unexplained [36]. Interestingly, this type of domain movement was proposed as possible due to "slippery" hydrophobic nature of the inter-domain interface [2] and suggested as the most likely [103] in 2006. The latter study even estimated the extent of domain rotation at ~20 ° based on molecular modeling and the length of the hinge in WT arrestins [103].

To gain an insight into the mechanism of JNK3 binding, we aligned the crystal structures of the basal conformation of arrestin-3 [31] and arrestin-2 [54] with a recent structure of a presumably "active" arrestin-2 [88] and compared the conformation of the three peptides, T1A, T3 and T6, identified as JNK3-binding elements (Fig 7). The folding of the key site, T1A, is remarkably similar in all three structures, whereas the conformations of T3 and T6 show slight differences (Fig. 7). This is consistent with previous observations that JNK3α2 binds both non-visual arrestins with similar affinities [18, 24] and JNK3α2 interaction is not particularly sensitive to arrestin conformation [24, 91]. Interestingly, the rotation of the two domains alters the relative positions of all three regions (Fig. 7A, B), suggesting that arrestin-3 binding to the receptor might change its affinity for JNK3α2. Although previously we demonstrated direct binding of JNK3α2 to free arrestin-3 in its basal conformation [18, 19] and here showed that JNK3α2 binds the arrestin3-receptor complex (Figs. 1,2), we could not compare JNK3α2 binding affinity in these two situations. To quantitatively evaluate the effect of receptor on the arrestin-3-JNK3α2 interaction, the affinity of this

binding needs to be measured, and the efficiency of scaffolding of ASK1-MKK4/7-JNK3α2 signaling cascade in the presence and absence of GPCRs must be quantitatively determined.

Our data with JNK3α2 (Fig. 4–6) support previously proposed model where each kinase in the ASK1-MKK4/7-JNK3 and c-Raf1-MEK1-ERK2 cascades binds both arrestin domains [17]. This is likely a universal mechanism of arrestin-mediated scaffolding of MAPK cascades, but it still does not explain how arrestins avoid assembling mismatched combinations of MAP kinases. One possibility is that the binding of one kinase significantly alters the recruitment of another. Indeed, the binding of ASK1 and JNK3 was shown to enhance MKK4 association with arrestin [3, 17]. We recently found that JNK3 binding to arrestin-3 differentially modulates the recruitment of the two upstream MAPKKs, MKK4 and MKK7, enhancing the binding of MKK4 while reducing that of MKK7 [19]. Although these results were obtained with kinases from the same module, the data suggest that interdependence of the binding of different partners likely contributes to the assembly of productive signaling complexes containing matching kinases.

Precise mapping of arrestin elements mediating its interactions with individual partners paves the way to the construction of arrestins where these interactions are selectively disabled or enhanced. These tools can be used for channeling cell signaling in the desired direction.

Conclusions

- Receptor-bound arrestin-3 interacts with JNK3α2
- JNK3α2 engages both domains of arrestin-3
- The first 25 residues in the N-domain contain the key JNK3α2 docking site
- JNK3α2 likely binds to more than one site on the C-domain
- The MBP fusions of arrestin-3 peptides are useful tools for the identification of the binding sites of other non-receptor partners

Acknowledgments

The authors are grateful to Dr. Keiji Tanaka, Tokyo Institute of Medical Science, for pMal-2T plasmid, and to Mr. J. Colon for technical assistance. Supported in part by NIH grants GM077561, GM081756, and EY011500 (VVG).

Abbreviations

GPCR	G protein-coupled receptor
JNK	c-Jun NH_2-terminal protein kinase
MAPK	mitogen-activated protein kinase
MKK or MAPKK	MAP kinase kinase
MAPKKK	MAP kinase kinase kinase
ASK1	Apoptosis signal-regulating kinase 1, a. k. a. mitogen-activated protein kinase kinase kinase 5 (MAP3K5)
MBP	maltose binding protein
WT	wild type
Rh*	light-activated unphosphorylated rhodopsin

P-Rh* light-activated phosphorylated rhodopsin

References

1. Carman CV, Benovic JL. Curr Opin Neurobiol. 1998; 8:335–344. [PubMed: 9687355]
2. Gurevich VV, Gurevich EV. Pharm Ther. 2006; 110:465–502.
3. McDonald PH, Chow CW, Miller WE, Laporte SA, Field ME, Lin FT, Davis RJ, Lefkowitz RJ. Science. 2000; 290:1574–1577. [PubMed: 11090355]
4. Luttrell LM, Roudabush FL, Choy EW, Miller WE, Field ME, Pierce KL, Lefkowitz RJ. Proc Natl Acad Sci U S A. 2001; 98:2449–2454. [PubMed: 11226259]
5. Bruchas MR, Macey TA, Lowe JD, Chavkin C. J Biol Chem. 2006; 281:18081–18089. [PubMed: 16648139]
6. DeFea KA. Annu Rev Physiol. 2007; 69:535–560. [PubMed: 17002593]
7. Kook S, Zhan X, Cleghorn WM, Benovic JL, Gurevich VV, Gurevich EV. Cell Death Diff. 2014; 21:172–184.
8. Shenoy SK, McDonald PH, Kohout TA, Lefkowitz RJ. Science. 2001; 294:1307–1313. [PubMed: 11588219]
9. Ahmed MR, Zhan X, Song X, Kook S, Gurevich VV, Gurevich EV. Biochemistry. 2011; 50:3749–3763. [PubMed: 21466165]
10. Xiao K, McClatchy DB, Shukla AK, Zhao Y, Chen M, Shenoy SK, Yates JR, Lefkowitz RJ. Proc Natl Acad Sci U S A. 2007; 104:12011–12016. [PubMed: 17620599]
11. Gurevich EV, Gurevich VV. Genome Biol. 2006; 7:236. [PubMed: 17020596]
12. Gurevich VV, Gurevich EV. Structure. 2003; 11:1037–1042. [PubMed: 12962621]
13. Sabapathy K. Prog Mol Biol Transl Sci. 2012; 106:145–169. [PubMed: 22340717]
14. Davis RJ. Cell. 2000; 103:239–252. [PubMed: 11057897]
15. Burack WR, Shaw AS. Curr Opin Cell Biol. 2000; 12:211–216. [PubMed: 10712921]
16. Good MC, Zalatan JG, Lim WA. Science. 2011; 332:680–686. [PubMed: 21551057]
17. Song X, Coffa S, Fu H, Gurevich VV. J Biol Chem. 2009; 284:685–695. [PubMed: 19001375]
18. Zhan X, Kaoud TS, Dalby KN, Gurevich VV. Biochemistry. 2011; 50:10520–10529. [PubMed: 22047447]
19. Zhan X, Kaoud TS, Kook S, Dalby KN, Gurevich VV. J Biol Chem. 2013; 288 in press.
20. Kook S, Zhan X, Kaoud TS, Dalby KN, Gurevich VV, Gurevich EV. J Biol Chem. 2014; 289 in press.
21. Gurevich VV, Gurevich EV. Cell Signal. 2012; 24:1899–1908. [PubMed: 22664341]
22. Gurevich VV, Gurevich EV. Expert Rev Mol Med. 2010; 12:e13. [PubMed: 20412604]
23. Miller WE, McDonald PH, Cai SF, Field ME, Davis RJ, Lefkowitz RJ. J Biol Chem. 2001; 276:27770–27777. [PubMed: 11356842]
24. Song X, Raman D, Gurevich EV, Vishnivetskiy SA, Gurevich VV. J Biol Chem. 2006; 281:21491–21499. [PubMed: 16737965]
25. Seo J, Tsakem EL, Breitman M, Gurevich VV. J Biol Chem. 2011; 286:27894–27901. [PubMed: 21715332]
26. Breitman M, Kook S, Gimenez LE, Lizama BN, Palazzo MC, Gurevich EV, Gurevich VV. J Biol Chem. 2012; 287:19653–19664. [PubMed: 22523077]
27. Pfleger KDG, Eidne KA. Nat Methods. 2006; 3:165–174. [PubMed: 16489332]
28. Pfleger KDG, Seeber RM, Eidne KA. Nat Protoc. 2006; 1:337–345. [PubMed: 17406254]
29. Gimenez LE, Kook S, Vishnivetskiy SA, Ahmed MR, Gurevich EV, Gurevich VV. J Biol Chem. 2012; 287:9028–9040. [PubMed: 22275358]
30. Gimenez LE, Vishnivetskiy SA, Gurevich VV. J Biol Chem. 2012; 287 in revision.
31. Zhan X, Gimenez LE, Gurevich VV, Spiller BW. J Mol Biol. 2011; 406:467–478. [PubMed: 21215759]

32. Gurevich VV, Benovic JL. Methods Enzymol. 2000; 315:422–437. [PubMed: 10736718]
33. Vishnivetskiy SA, Raman D, Wei J, Kennedy MJ, Hurley JB, Gurevich VV. J Biol Chem. 2007; 282:32075–32083. [PubMed: 17848565]
34. Vishnivetskiy SA, Baameur F, Findley KR, Gurevich VV. J Biol Chem. 2013; 288:11741–11750. [PubMed: 23476014]
35. Vishnivetskiy SA, Chen Q, Palazzo MC, Brooks EK, Altenbach C, Iverson TM, Hubbell WL, Gurevich VV. J Biol Chem. 2013; 288:11741–11750. [PubMed: 23476014]
36. Kim M, Vishnivetskiy SA, Van Eps N, Alexander NS, Cleghorn WM, Zhan X, Hanson SM, Morizumi T, Ernst OP, Meiler J, Gurevich VV, Hubbell WL. Proc Nat Acad Sci USA. 2012; 109:18407–18412. [PubMed: 23091036]
37. Coffa S, Breitman M, Hanson SM, Callaway K, Kook S, Dalby KN, Gurevich VV. PLoS One. 2011; 6:e28723. [PubMed: 22174878]
38. Vishnivetskiy SA, Hirsch JA, Velez M-G, Gurevich YV, Gurevich VV. J Biol Chem. 2002; 277:43961–43968. [PubMed: 12215448]
39. Hanson SM, Cleghorn WM, Francis DJ, Vishnivetskiy SA, Raman D, Song X, Nair KS, Slepak VZ, Klug CS, Gurevich VV. J Mol Biol. 2007 in press.
40. Schleicher A, Kuhn H, Hofmann KP. Biochemistry. 1989; 28:1770–1775. [PubMed: 2719933]
41. Hanson SM, Francis DJ, Vishnivetskiy SA, Kolobova EA, Hubbell WL, Klug CS, Gurevich VV. Proc Natl Acad Sci U S A. 2006; 103:4900–4905. [PubMed: 16547131]
42. Vishnivetskiy SA, Francis DJ, Van Eps N, Kim M, Hanson SM, Klug CS, Hubbell WL, Gurevich VV. J Mol Biol. 2010; 395:42–54. [PubMed: 19883657]
43. Zhuang T, Chen Q, Cho M-K, Vishnivetskiy SA, Iverson TI, Gurevich VV, Hubbell WL. Proc Nat Acad Sci USA. 2013; 110:942–947. [PubMed: 23277586]
44. Gurevich VV. J Biol Chem. 1998; 273:15501–15506. [PubMed: 9624137]
45. Celver J, Vishnivetskiy SA, Chavkin C, Gurevich VV. J Biol Chem. 2002; 277:9043–9048. [PubMed: 11782458]
46. Carter JM, Gurevich VV, Prossnitz ER, Engen JR. J Mol Biol. 2005; 351:865–878. [PubMed: 16045931]
47. Kovoor A, Celver J, Abdryashitov RI, Chavkin C, Gurevich VV. J Biol Chem. 1999; 274:6831–6834. [PubMed: 10066734]
48. Gurevich VV, Benovic JL. J Biol Chem. 1993; 268:11628–11638. [PubMed: 8505295]
49. Wilden U, Wüst E, Weyand I, Kühn H. FEBS Lett. 1986; 207:292–295. [PubMed: 3770202]
50. Barak LS, Ferguson SS, Zhang J, Caron MG. J Biol Chem. 1997; 272:27497–27500. [PubMed: 9346876]
51. Levchenko A, Bruck J, Sternberg PW. Proc Natl Acad Sci U S A. 2000; 97:5818–5823. [PubMed: 10823939]
52. Levchenko A, Bruck J, Sternberg PW. Syst Biol (Stevenage). 2004; 1:139–148. [PubMed: 17052124]
53. Granzin J, Wilden U, Choe HW, Labahn J, Krafft B, Buldt G. Nature. 1998; 391:918–921. [PubMed: 9495348]
54. Han M, Gurevich VV, Vishnivetskiy SA, Sigler PB, Schubert C. Structure. 2001; 9:869–880. [PubMed: 11566136]
55. Hirsch JA, Schubert C, Gurevich VV, Sigler PB. Cell. 1999; 97:257–269. [PubMed: 10219246]
56. Milano SK, Pace HC, Kim YM, Brenner C, Benovic JL. Biochemistry. 2002; 41:3321–3328. [PubMed: 11876640]
57. Sutton RB, Vishnivetskiy SA, Robert J, Hanson SM, Raman D, Knox BE, Kono M, Navarro J, Gurevich VV. J Mol Biol. 2005; 354:1069–1080. [PubMed: 16289201]
58. Ohguro H, Palczewski K, Walsh KA, Johnson RS. Protein Sci. 1994; 3:2428–2434. [PubMed: 7756996]
59. Gurevich VV, Dion SB, Onorato JJ, Ptasienski J, Kim CM, Sterne-Marr R, Hosey MM, Benovic JL. J Biol Chem. 1995; 270:720–731. [PubMed: 7822302]
60. Gurevich VV, Benovic JL. J Biol Chem. 1995; 270:6010–6016. [PubMed: 7890732]

61. Gurevich VV, Benovic JL. Mol Pharmacol. 1997; 51:161–169. [PubMed: 9016359]
62. Hanson SM, Gurevich VV. J Biol Chem. 2006; 281:3458–3462. [PubMed: 16339758]
63. Dinculescu A, McDowell JH, Amici SA, Dugger DR, Richards N, Hargrave PA, Smith WC. J Biol Chem. 2002; 277:11703–11708. [PubMed: 11809770]
64. Pulvermuller A, Schroder K, Fischer T, Hofmann KP. J Biol Chem. 2000; 275:37679–37685. [PubMed: 10969086]
65. Vishnivetskiy SA, Hosey MM, Benovic JL, Gurevich VV. J Biol Chem. 2004; 279:1262–1268. [PubMed: 14530255]
66. Vishnivetskiy SA, Gimenez LE, Francis DJ, Hanson SM, Hubbell WL, Klug CS, Gurevich VV. J Biol Chem. 2011; 286:24288–24299. [PubMed: 21471193]
67. Zhuang T, Vishnivetskiy SA, Gurevich VV, Sanders CR. Biochemistry. 2010:10473–10485. [PubMed: 21050017]
68. Li X, Macleod R, Dunlop AJ, Edwards HV, Advant N, Gibson LC, Devine NM, Brown KM, Adams DR, Houslay MD, Baillie GS. FEBS Lett. 2009; 583:3310–3316. [PubMed: 19782076]
69. Vishnivetskiy SA, Schubert C, Climaco GC, Gurevich YV, Velez M-G, Gurevich VV. J Biol Chem. 2000; 275:41049–41057. [PubMed: 11024026]
70. Song X, Vishnivetskiy SA, Gross OP, Emelianoff K, Mendez A, Chen J, Gurevich EV, Burns ME, Gurevich VV. Curr Biol. 2009; 19:700–705. [PubMed: 19361994]
71. Pan L, Gurevich EV, Gurevich VV. J Biol Chem. 2003; 278:11623–11632. [PubMed: 12525498]
72. Vishnivetskiy SA, Ostermaierm MK, Singhal A, Panneels V, Homan KT, Glukhova A, Sligar SG, Tesmer JJ, Schertler GF, Standfuss J, Gurevich VV. Cell Signal. 2013; 25:2155–2162. [PubMed: 23872075]
73. Shukla AK, Xiao K, Lefkowitz RJ. Trends Biochem Sci. 2011; 36:457–469. [PubMed: 21764321]
74. Attramadal H, Arriza JL, Aoki C, Dawson TM, Codina J, Kwatra MM, Snyder SH, Caron MG, Lefkowitz RJ. J Biol Chem. 1992; 267:17882–17890. [PubMed: 1517224]
75. Sterne-Marr R, Gurevich VV, Goldsmith P, Bodine RC, Sanders C, Donoso LA, Benovic JL. J Biol Chem. 1993; 268:15640–15648. [PubMed: 8340388]
76. Gurevich VV, Gurevich EV. Prog Mol Biol Transl Sci. 2013; 118:57–92. [PubMed: 23764050]
77. Kim YM, Benovic JL. J Biol Chem. 2002; 277:30760–30768. [PubMed: 12070169]
78. Xiao K, Shenoy SK, Nobles K, Lefkowitz RJ. J Biol Chem. 2004; 279:55744–55753. [PubMed: 15501822]
79. Bhandari D, Trejo J, Benovic JL, Marchese A. J Biol Chem. 2007; 282:36971–36979. [PubMed: 17947233]
80. Wu N, Hanson SM, Francis DJ, Vishnivetskiy SA, Thibonnier M, Klug CS, Shoham M, Gurevich VV. J Mol Biol. 2006; 364:955–963. [PubMed: 17054984]
81. Goodman OB, Krupnick JG, Santini F, Gurevich VV, Penn RB, Gagnon AW, Keen JH, Benovic JL. Nature. 1996; 383:447–450. [PubMed: 8837779]
82. Laporte SA, Oakley RH, Holt JA, Barak LS, Caron MG. J Biol Chem. 2000; 275:23120–23126. [PubMed: 10770944]
83. Moaven H, Koike Y, Jao CC, Gurevich VV, Langen R, Chen J. Proc Nat Acad Sci USA. 2013; 110:9463–9468. [PubMed: 23690606]
84. Hanson SM, Francis DJ, Vishnivetskiy SA, Klug CS, Gurevich VV. J Biol Chem. 2006; 281:9765–9772. [PubMed: 16461350]
85. Baillie GS, Adams DR, Bhari N, Houslay TM, Vadrevu S, Meng D, Li X, Dunlop A, Milligan G, Bolger GB, Klussmann E, Houslay MD. Biochem J. 2007; 404:71–80. [PubMed: 17288540]
86. Meng D, Lynch MJ, Huston E, Beyermann M, Eichhorst J, Adams DR, Klusmann E, Houslay MD, Baillie GS. J Biol Chem. 2009; 284:11425–11435. [PubMed: 19153083]
87. Kim YJ, Hofmann KP, Ernst OP, Scheerer P, Choe HW, Sommer ME. Nature. 2013; 497:142–146. [PubMed: 23604253]
88. Shukla AK, Manglik A, Kruse AC, Xiao K, Reis RI, Tseng WC, Staus DP, Hilger D, Uysal S, Huang LY, Paduch M, Tripathi-Shukla P, Koide A, Koide S, Weis WI, Kossiakoff AA, Kobilka BK, Lefkowitz RJ. Nature. 2013; 497:137–141. [PubMed: 23604254]

89. Masterson LR, Bortone N, Yu T, Ha KN, Gaffarogullari EC, Nguyen O, Veglia G. Protein Expr Purif. 2009; 64:231–236. [PubMed: 19027069]

90. Martin EL, Rens-Domiano S, Schatz PJ, Hamm HE. J Biol Chem. 1996; 271:361–366. [PubMed: 8550587]

91. Song X, Gurevich EV, Gurevich VV. J Neurochem. 2007; 103:1053–1062. [PubMed: 17680991]

92. Gurevich VV, Benovic JL. J Biol Chem. 1992; 267:21919–21923. [PubMed: 1400502]

93. Choi WS, Abel G, Klintworth H, Flavell RA, Xia Z. J Neuropathol Exp Neurol. 2010; 69:511–520. [PubMed: 20418776]

94. Flemming A. Nat Rev Drug Discov. 2012; 11:829. [PubMed: 23123935]

95. Yoon SO, Park DJ, Ryu JC, Ozer HG, Tep C, Shin YJ, Lim TH, Pastorino L, Kunwar AJ, Walton JC, Nagahara AH, Lu KP, Nelson RJ, Tuszynski MH, Huang K. Neuron. 2012; 75:824–837. [PubMed: 22958823]

96. Perrin V, Dufour N, Raoul C, Hassig R, Brouillet E, Aebischer P, Luthi-Carter R, Déglon N. Exp Neurol. 2009; 215:191–200. [PubMed: 19022249]

97. Antoniou X, Falconi M, Di Marino D, Borsello T. J Alzheimers Dis. 2011; 24:633–642. [PubMed: 21321401]

98. Shoemaker BA, Portman JJ, Wolynes PG. Proc Natl Acad Sci U S A. 2000; 97:8868–8873. [PubMed: 10908673]

99. Sugase K, Dyson HJ, Wright PE. Nature. 2007; 447:1021–1025. [PubMed: 17522630]

100. Gurevich VV, Gurevich EV. Trends Pharmacol Sci. 2004; 25:105–111. [PubMed: 15102497]

101. Feuerstein SE, Pulvermüller A, Hartmann R, Granzin J, Stoldt M, Henklein P, Ernst OP, Heck M, Willbold D, Koenig BW. Biochemistry. 2009; 48:10733–10742. [PubMed: 19835414]

102. Kirchberg K, Kim TY, Möller M, Skegro D, Dasara Raju G, Granzin J, Büldt G, Schlesinger R, Alexiev U. Proc Nat Acad Sci USA. 2011; 108:18690–18695. [PubMed: 22039220]

103. Modzelewska A, Filipek S, Palczewski K, Park PS. Cell Biochem Biophys. 2006; 46:1–15. [PubMed: 16943619]

Highlights

- Receptor-associated arrestin-3 binds JNK3α2
- JNK3α2 interacts with both domains of arrestin-3
- The first 25 residues of arrestin-3 contain the key JNK3α2 binding site
- Distinct arrestin-3 elements mediate binding and activation of JNK3α2

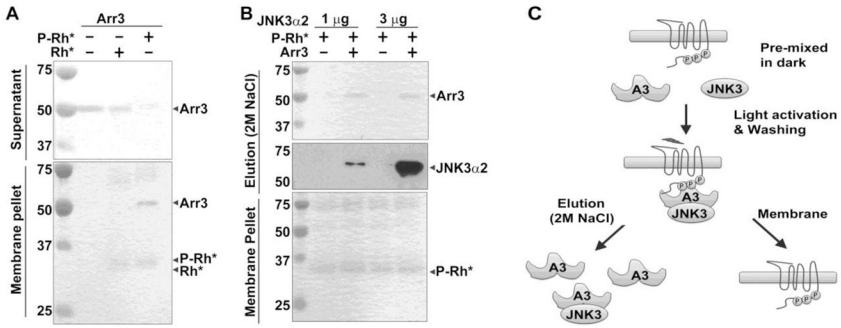

Fig. 1. Rhodopsin-associated arrestin-3 binds JNK3α2

A. Coomassie-stained SDS-PAGE gels showing purified arrestin-3 in supernatant (upper panel) or pellet (lower panel) upon incubation without (−) or with (+) light-activated unphosphorylated Rh* or P-Rh*. **B.** Upper panel, Coomassie-stained SDS-PAGE gel showing arrestin-3 eluted by 2 M NaCl, 50 mM HEPES, pH 7.3; middle panel, Western blot of JNK3α2 in the eluate; lower panel, Coomassie-stained SDS-PAGE gel showing P-Rh* in the pellet. Note that JNK3α2 does not bind P-Rh* in the absence of arrestin-3. **C.** A schematic of the experiment designed to detect direct interaction between P-Rh*-bound arrestin-3 (A3) and JNK3α2 (JNK3). Two-dimensional schematic of rhodopsin with seven trans-membrane helices and three phosphates (P) on the C-terminus is shown.

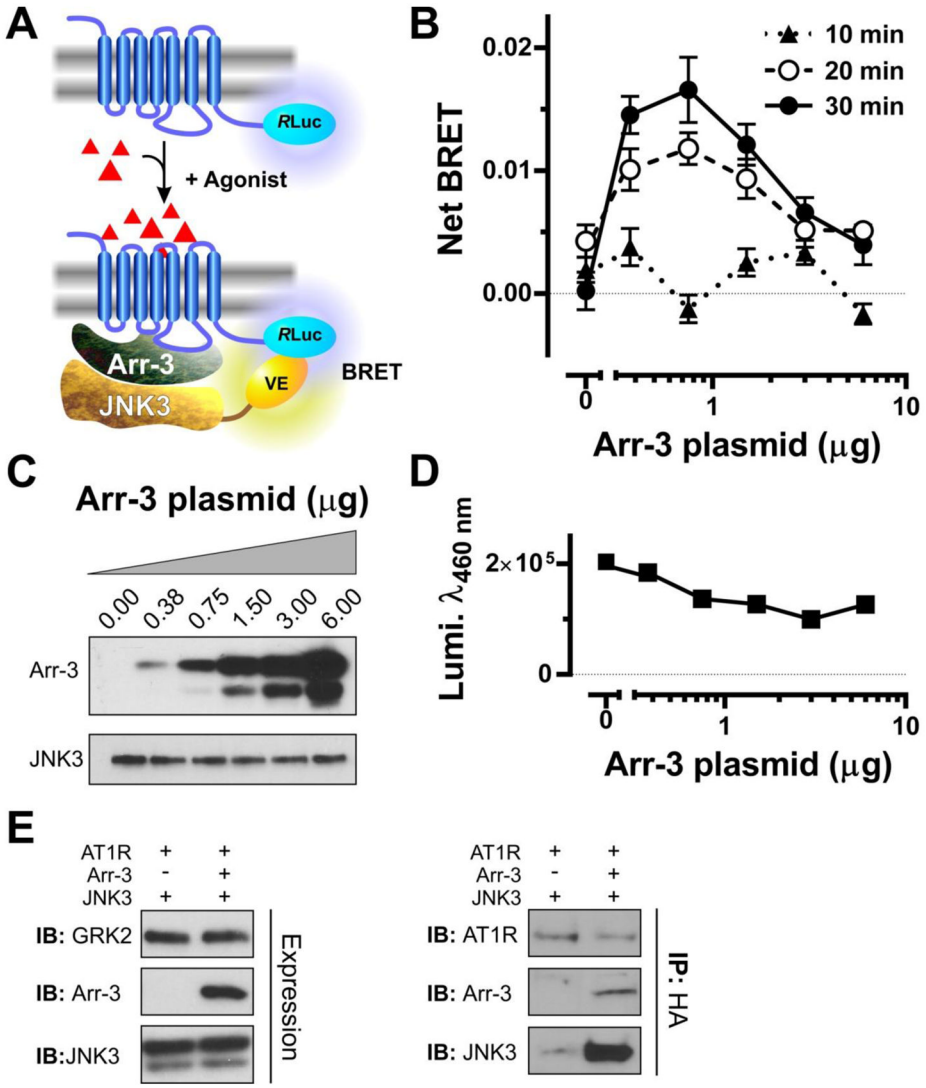

Fig. 2. Receptor-bound arrestin-3 retains the ability to bind JNK3α2

A. BRET assay to evaluate the ability of arrestin-3 associated with AT1R to bind JNK3α2. AT1R was tagged with *Renilla* luciferase 8 (RLuc) at the C-terminus, JNK3α2 was tagged at the N-terminus with Venus (VE-JNK3), and these proteins were co-expressed with arrestin-3 in COS-7 cells. **B.** Net BRET (agonist-induced increase in BRET signal between AT1R-*R*Luc8 and VE-JNK3) was determined at 10 min (filled triangles; dotted line), 20 min (open circles; dashed line), and 30 min (filled circles; solid line) after angiotensin II stimulation. Net BRET is the difference between BRET ratios in the presence and absence of 1 μM angiotensin II. Means ± SEM of a typical experiment out of three performed with eight replicates in each. **C.** Western blots showing the expression of VE-JNK3 and progressively increased expression of arrestin-3 as a function of the amounts of arrestin-3 encoding plasmid. **D.** The expression of AT1R-*R*Luc8 is shown as peak luminescence at 460 nm. **E.** HEK-293A cells were transfected with HA-AT1R-RLuc, Flag-JNK3α2 and GRK2 with or without arrestin-3. Cell lysates (10 μg total protein) were analyzed by Western blot using indicated antibodies. HA-tagged AT1R-*R*luc8 was immunoprecipitated (IP) by an anti-HA antibody from cell lysates. The immunoprecipitate was analyzed by Western blot

using anti-HA, arrestin-3 (Arr-3), or JNK3 antibodies. AT1R was only detected in the immunoprecipitated samples because of its low expression.

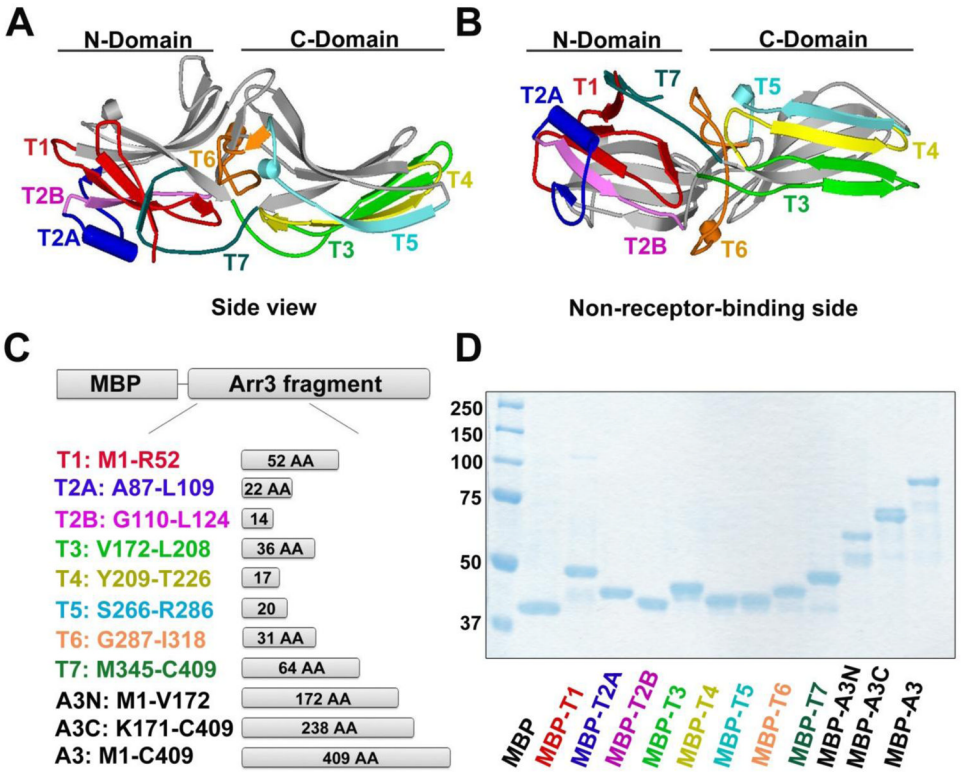

Fig. 3. Design and purification of maltose binding protein (MBP)-fusion proteins containing arrestin-3 elements

A, B. Side view (**A**) and view from non-receptor-binding side (**B**) of the basal conformation of arrestin-3 (PDB: 3P2D; [31]) with the eight arrestin-3 peptide fragments used here shown in different colors. **C.** The schematic of the MBP-fusion proteins containing arrestin-3 peptide fragments. **D.** Coomassie-stained SDS-PAGE gel showing the purity of MBP-fusion proteins (1 μg of each protein was loaded). Molecular weights of the MBP fusion proteins were: MBP (with linker and additional residues), 44.7 kDa; MBP-T1, 49.4 kDa; MBP-T2A, 46.2 kDa; MBP-T2B, 45,3 kDA; MBP-T3, 47.6 kDa; MBP-T4, 45,9 kDa; MBP-T5, 46.1 kDa; MBP-T6, 45.6 kDa; MBP-T7, 51.0 kDa; MBP-A3N, 63.0 kDa; MBP-A3C, 70.3 kDa; MBP-A3, 89,6 kDa. The same color-coding is used in panels **A**–**D**.

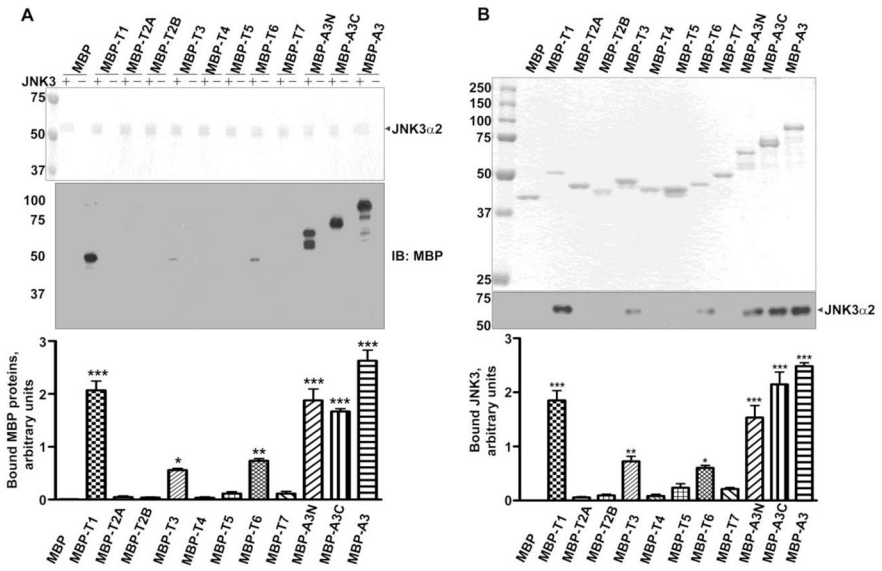

Fig. 4. Multiple binding sites in both domains mediate JNK3α2 interaction with arrestin-3

A. Identification of the JNK3α2 binding sites on arrestin-3 by His-tag pull-down. Upper panel, Coomassie-stained SDS-PAGE gel showing the JNK3α2 retained by Ni-NTA column; lower panel, Western blot of the MBP proteins in the eluates from the indicated columns and bar graph showing the quantification of the Western blot. Means ± SD (n = 4) of the relative intensity of bands are shown (*, $p<0.05$: **, $p<0.01$; ***, $p<0.001$, as compared to MBP control). **B.** Identification of the JNK3α2 binding sites on arrestin-3 by MBP pull-down. MBP and MBP-arrestin-3 fusion protein were used as negative and positive controls, respectively. Upper panel, Coomassie-stained SDS-PAGE gel showing the MBP proteins retained by amylose column; lower panel, Western blot of the JNK3α2 in the eluates from the indicated columns and bar graph showing the quantification of the Western blot. Means ± SD (n = 4) of the relative intensity of bands are shown (*, $p<0.05$: **, $p<0.01$; ***, $p<0.001$, as compared to MBP control).

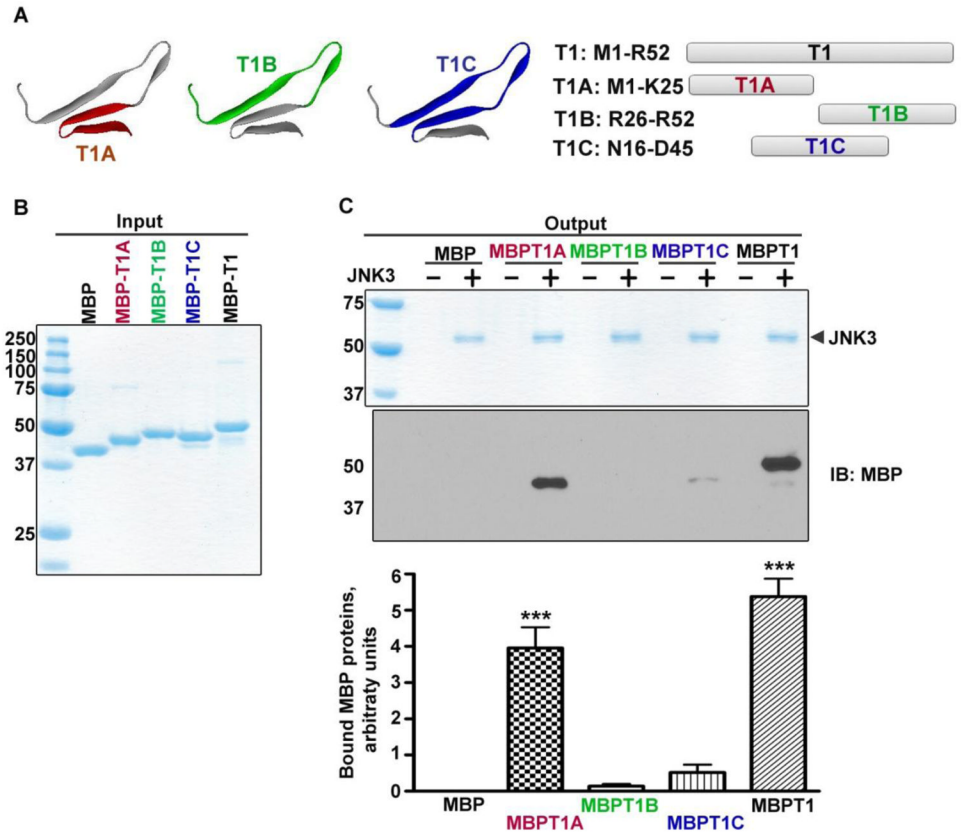

Fig. 5. The first 25 residues in the N-domain include the primary JNK3α2 binding site

A. The structures of three fragments within T1 peptide (based on PDB: 3P2D; [31]): T1A (red) containing the first 25 residues, T1B (green) containing the next 27 residues, and T1C (blue) including 26 residues overlapping with both T1A and T1B. **B.** The purity of the MBP proteins used in the pull-down assay shown in **C**. The molecular weights of the fusion proteins were: MBP (with linker and additional residues), 44.7 kDa; MBP-T1A, 46.2 kDa; MBP-T1B, 46.8 kDa; MBP-T1C, 46.6 kDa; MBP-T1, 49.4 kDa. **C.** The binding of MBP-T1A, T1B and T1C to JNK3α2 was measured by His-tag pull-down and compared with same amount of MBP and MBP-T1, which served as negative and positive controls, respectively. Upper panel, Coomassie-stained SDS-PAGE gel showing the JNK3α2 retained by Ni-NTA column; lower panel, Western blot of MBP fusion proteins in the eluates from the indicated columns and bar graph showing the quantification of the Western blot; means ± SD (n = 3) of the relative intensity of bands are shown (***, $p<0.001$, as compared to MBP control).

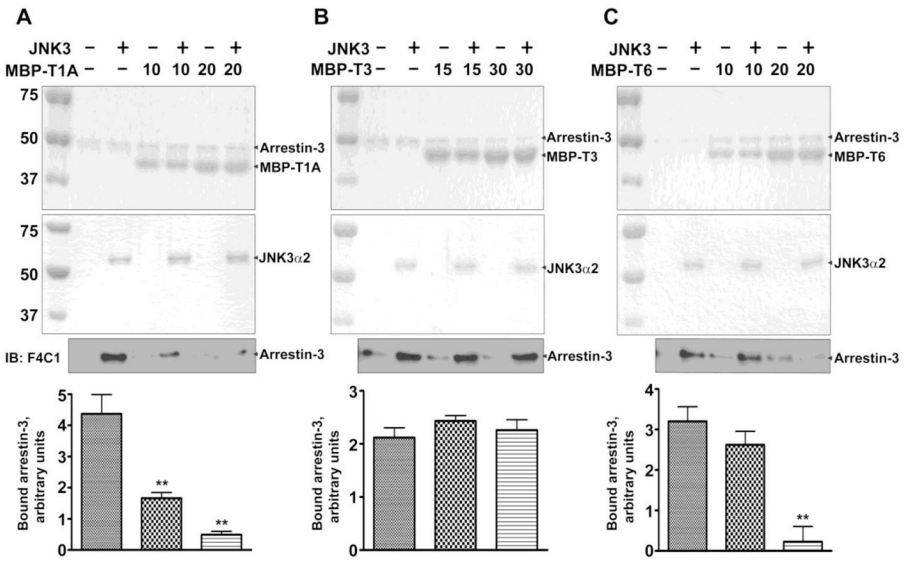

Fig. 6. T1A and T6 fragments significantly inhibit the interaction between arrestin-3 and JNK3α2

A–C. The effects of MBP-T1A, T3 and T6 on the interaction of arrestin-3 with JNK3α2 were analyzed by His-tag pull-down. **A.** Arrestin-3/JNK3α2 interaction was decreased by MBP-T1A. Upper panel, Coomassie-stained gel of input of prey proteins (arrestin-3 and MBP-T1A); middle panel, Coomassie-stained gel of output of bait protein JNK3α2; lower panel, Western blot of the JNK3α2 in the eluates from the indicated columns. **B.** MBP-T3 did not inhibit arrestin-3/JNK3α2 interaction. Upper panel, Coomassie-stained gel of input of prey proteins (arrestin-3 and MBP-T3); middle panel, Coomassie-stained gel of output of bait protein JNK3α2; lower panel, Western blot of the JNK3α2 in the eluates from the indicated columns. **C.** Arrestin-3/JNK3α2 interaction was decreased by MBP-T6. Upper panel, Coomassie-stained gel of input of prey proteins (arrestin-3 and MBP-T6); middle panel, Coomassie-stained gel of output of bait protein JNK3α2; lower panel, Western blot of the JNK3α2 in the eluates from the indicated columns and bar graph showing the quantification of the Western blot; means ± SD (n = 3) of the relative intensity of bands are shown (**, $p<0.01$, as compared to MBP control).

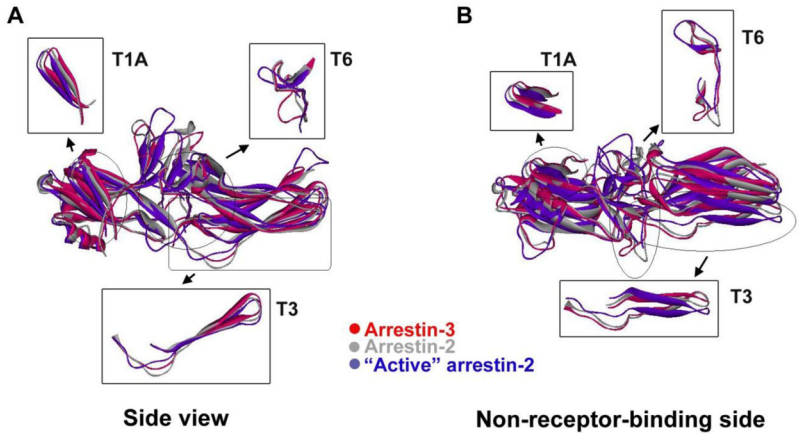

Fig. 7. The localization of JNK3α2 binding sites on non-visual arrestins

A, B. Alignments of the crystal structures of the basal conformation of arrestin-3 (red) (PDB: 3P2D; [31]) with basal (grey) (PDB: 1G4M; [54]) and "active" (blue) (PDB: 4JQI; [88]) conformations of arrestin-2. Side view (**A**) and the view from non-receptor-binding side (**B**) are shown. The positions and conformations of T1A, T3 and T6 peptides implicated in JNK3α2 binding are shown.